MEASUREMENT OF ATOMIC OSCILLATOR STRENGTHS IN YTTERBIUM BY OBSERVATION OF COHERENT RABI OSCILLATIONS OF EXCITED-STATE POPULATIONS*

C. Haynam, B. Comaskey, E. Worden, J. Paisner

UCRL--96778

DE87 011326

ABSTRACT

We have used two methods to measure the oscillator strength of the transition between the ground and 17992 cm^{-1} level in ^{174}Yb. The first technique involves exciting the transition with a laser pulse that is nearly time-bandwidth limited, of uniform intensity, and has a reproducible shape from shot to shot. The population left in the excited state after the pulse varies sinusoidally with a period that depends on the integral over time of the electric field amplitude and the transition oscillator strength. These are the Rabi oscillations that are predicted by application of the Schrodinger equation to the two-level atom. The excited-state population is probed using a two-step photoionization to the continuum. The electric field amplitude is determined from the temporal profile and the intensity of the laser pulse. The second method involves observation of the polarization rotation of a set of degenerate sublevels brought about by a light-shift laser. One sublevel ($m_j = 0$) of the $J = 1$ level at 17992 cm^{-1} is populated by a linearly polarized laser. A second copropagating light-shift laser, which is linearly polarized at an angle to the first laser, is tuned between 7.5 and 30 GHz off-resonance with the transition. The light-shift laser causes population to be promoted into the $m_j = \pm 1$ levels through the virtual $J = 0$, $m_j = 0$ level. Two linearly polarized photoionizing lasers photoionize the population only from the $m_j = \pm 1$ levels. The photoion signal oscillates cosinusoidally with a period that depends only on the integrated pulse intensity, the laser detuning, and the transition oscillator strength. Finally, polarization selectivity has been shown experimentally to allow selective photoionization of the odd isotopes of ytterbium using broadband lasers.

*Work performed under the auspices of the U.S. Department of Energy by the Lawrence Livermore National Laboratory under Contract W-7405-Eng-48.

INTRODUCTION

Ytterbium is a nearly ideal system to test new techniques for measuring transition oscillator strengths. The ground-state electronic configuration of $(4f^{14}6s^2)$ results in an even parity $^1S_0$ state. The spectroscopic parameters of the lowest energy J = 1 odd parity $(6s6p)^3P_1$ level at 17992 cm^{-1} are known, including lifetime (875 ns)[1] and a branching ratio of one to the $(6s^2)$ $^1S_0$ level. We shall discuss two techniques to measure oscillator strengths and apply them to the 555.6 nm $(6s^2)^1S_0 - (6s6p)^3P_1$ transition. The first technique observes the population oscillations of a two-level system due to resonant laser excitation. The measurement of the oscillation frequency vs integrated laser electric field intensity allows determination of the transition oscillator strength. The second method is similar to the inverse hook method developed by Wijngaarden et al.[2] Population is promoted to the $m_j = 0$ sublevel of the J = 1 state with a linearly polarized resonant pulse at 555.6 nm. A second off-resonant laser linearly polarized at an angle to the state preparation laser causes the population to flow into the $m_j = \pm 1$ sublevels. We observe population oscillations in these two sublevels. The measurement of oscillation frequency vs integrated laser fluence and laser detuning permits the determination of oscillator strength. In both cases the photoion signal resulting from a two-step photoionization process is used to observe population oscillations.

EXPERIMENTS AND RESULTS

The population oscillations that result when two atomic states are coupled through resonant laser excitation can be used to measure the oscillator strength of the transition. Detection of this population oscillation can be obtained by many methods. Detection by photoionization was first done by Scarl et al.[3] The photoionization pathway we use in Yb is shown in Fig. 1. This is a three-step photoionization using linearly polarized lasers. The first step couples only two m_j levels forming a two-level system. The experimental apparatus is shown in Fig. 2. The 555.6-nm laser is produced by pulse amplification of an actively stabilized ring dye laser. Long-term

stability of the central frequency is monitored with a 150-MHz confocal etalon. The laser's fluence is varied with a Pockels cell. Amplified spontaneous emission is filtered from the pulse using a low-finesse flat-flat etalon. The resultant beam was tightly collimated, passed through a 0.2-mm pinhole, and allowed to diffract for roughly 3 m to the interaction region. The central lobe of the Airy pattern created in this fashion is nearly 2 cm in diam. The fluence of each pulse of this laser is measured with a Molectron pyroelectric detector and boxcar and recorded in a computer. At the end of a measurement a number of temporal pulse shapes are digitized on a fast oscilloscope. The second-step laser at 458.2 nm was generated by nitrogen pumping a dye laser and was spectrally ~15 GHz wide. This laser was tightly focused to about 1 mm on the central portion of the Airy pattern. All atoms in this spatial region see a very nearly uniform 555.6 nm laser intensity. A broadband third-step laser at 566.9 nm generated by a frequency doubled Nd:YAG pumped dye laser completes the three-step photoionization. An atomic beam is generated by resistively heating a tungsten filament, which in turn radiatively heats a tungsten crucible filled with Yb. The photoionization region is magnetically shielded using a mu metal box. The photoions pass through a quadrupole mass spectrometer that selects the nuclear spin free ^{174}Yb isotope. The photoion signal is recorded each shot, sorted into the appropriate laser intensity increment, and averaged with any other previously recorded samples in that increment.

The solution for the two-level on-resonant atom is shown in Fig. 3. The 555.6-nm laser is nearly time-bandwidth limited (±10%). The spectral width of about 100 MHz is larger than the 75 MHz Doppler width of the atomic beam. As a result, the on-resonant approximation is valid. The population promoted to the $m_j = 1$ $J = 1$ level depends only on the integral of the electric field and the oscillator strength of the transition. This integral can be deduced from the laser fluence and the temporal profile of the laser pulse (Fig. 4), assuming constant phase throughout the pulse (no chirp). For our Quanta-Ray DCR2 system, the normalized integral of the square root of the intensity profile varies by less than 10% from pulse to pulse. This implies that the phase angle of the sinusoid is proportional to the square root of the intensity. The experimentally observed oscillations are shown in Fig. 5. The

dramatic oscillations show total elimination of ion signal when pi, two pi, and three pi pulses excite the atom. From these data we calculate an oscillator strength of $(1.82 \pm 0.36) \times 10^{-2}$. From branching ratio and lifetime measurements, the oscillator strength of this transition is known to be 1.59×10^{-2}.

The second method used to measure oscillator strength depends on polarization selectivity to discriminate between the populations in the $m_j = 0$ level and the $m_j = \pm 1$ levels. The linearly polarized λ_1 laser promotes the population only to the $m_j = 0$ sublevel of the 17992 cm^{-1} level in the spin zero ^{174}Yb atom. Due to selection rules, a second linearly parallel polarized laser will promote no population to the (6s6d) $^3D_1$ level at 39808 cm^{-1}. This selection rule does not apply to the two odd isotopes with nonzero nuclear spin. The experimental demonstration of this is shown in Fig. 6. The lower figure shows the photoion signal as a function of mass when broadband lasers are used to excite all isotopes of Yb and polarization selectivity is eliminated by orienting λ_2 orthogonal to λ_1 and λ_3. Under these conditions all the isotopes of Yb are observed to photoionize. The top portion of Fig. 6 shows the results of reorienting the second step laser so that all three steps are parallel polarized. Less than 3% of the original ^{174}Yb photoion signal is observed, but the odd isotopes are readily photoionized. This selective photoionization of odd isotopes using polarization selectivity was first suggested by Balling and Wright in 1976.[4]

The excitation scheme for the off-resonant experiment is shown in Fig. 7. All lasers are temporally separated. The λ_Δ laser comes between the λ_1 and λ_2 laser temporally and is again generated by pulse amplification of a ring dye laser. This λ_Δ laser nearly copropagates with λ_1 and counterpropagates with respect to λ_2 (copropagation of λ_1 and λ_2 can also be used). For most of the experiments the angle between the electric field vectors of λ_Δ and λ_1 was fixed at 54.7° (magic angle excitation), but other orientations were used. The population oscillation period is not expected to depend on this angle. Only the population that has been shifted into the $m_j = \pm 1$ levels by the light-shift laser λ_Δ can be subsequently photoionized by λ_2 and λ_3. The analysis of this process is shown in Fig. 8. The original quantization axis in the system (z axis) is defined by the λ_1 electric field vector.

The λ_Δ laser is detuned slightly from resonance and couples the $m_j = \pm 1$ states to the 0 state. In this picture, a two-photon process first promotes the population to the $J = 0$ level and then redistributes the population into the $J = 1$ level. The level amplitudes and populations oscillate in time. A more convenient way to look at this system is to rotate the coordinate system using the unitary representation of the rotation group (Fig. 9). Using the notation of Tinkham,[5] the transform is $D^{(1)}(0,\beta,0)$. This transformation aligns the λ_Δ laser with the quantization axis. The time evolution of the system can now be solved as a two-level atom excited far off-resonance.

The far off-resonance condition allows considerable simplification in the calculation of each state's time evolution (Fig. 10). Very little population is ever promoted to the $J = 0$ state from the $J = 1$ state, and very little of the population remaining in the $J = 0$ state after the λ_1 pulse is promoted to the $J = 1$ level by the λ_Δ laser. The result is that the magnitude of the $m_j = 0$ $J = 0$ level's state amplitude remains constant, but its phase varies with time. The reverse transformation mixes the primed states, giving rise to time-dependent state populations (Fig. 11). A simple expression is derived that relates the population in each of the $m_j = \pm 1$ levels to the total fluence in the λ_Δ pulse:

$$P_1 = \sin^2(\beta)\cos^2(\beta)[1 - \cos(f_{\ell u} I/(4\pi\Delta)],$$

where I is the fluence in photons/cm^2. With higher J systems, each m_j component's phase would evolve separately in time, with only the Rabi rate changing between components.

In order to compare the exact solution with the adiabatic approximation, a number of computer simulations, which solve for the time-dependent state populations, were implemented by numeric integration of the Schrodinger equation. A pulse of uniform intensity 6 ns in duration was used. The integrated fluence in the pulse was adjusted to yield two population oscillation cycles in the adiabatic approximation. As the detuning is reduced, the ratio of Rabi rate to the detuning (Ω/Δ) increases and the adiabatic approximation becomes poor (Figs. 12-14). For detunings of 7.5 GHz and larger, the adiabatic approximation holds reasonably well.

Experimental results are shown in Fig. 15. Laser detunings varied from 7.5 GHz to 30 GHz. The fluence required to give one oscillation at 30 GHz detuning is over a thousand times larger than the fluence required to observe one oscillation using the on-resonant measurement technique (Fig. 5). In order to reach higher fluences, a larger 0.4-mm pinhole was used. As a result, the spatial uniformity of the beam was sacrificed. The resulting distribution of intensities was modeled assuming a uniform distribution of intensities ranging from ±15% centered on the average. The solid line shows the results of a nonlinear least-squares fit to the data, with the damping of the oscillations due to fluence variations. Within experimental limits, agreement is found with the literature value of the oscillator strength.

References

[1] M. Gustaasson, H. Lundberg, L. Nilsson, and S. Svanberg, J. Opt. Soc. Am. 69, 984 (1979).

[2] W. A. van Wijngaarden, K. Bonn, W. Happer, E. Miron, D. Schreiber, and T. Arisawa, Phys. Rev. Lett. 56, 2024 (1986).

[3] D. Scarl, L. A. Hackel, M. A. Johnson, and M. C. Rushford, Phys. Rev. A 24, 883 (1981).

[4] L. C. Balling and J. J. Wright, Appl. Phys. Lett. 29, 411 (1976).

[5] M. Tinkham, Group Theory and Quantum Mechanics, McGraw-Hill, 111 (1964).

Excitation sequences for oscillator strength measurements observing on resonant Rabi oscillations

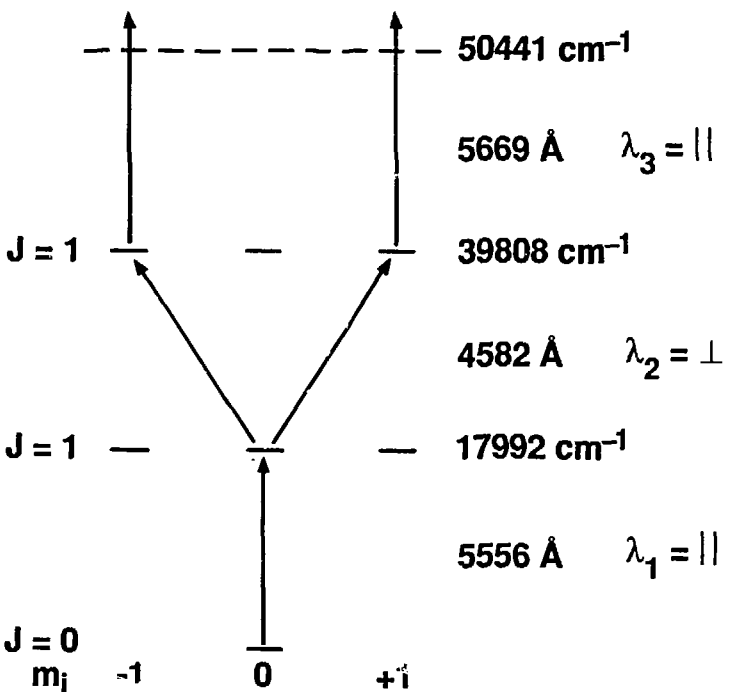

All lasers pass through atomic vapor temporally separated

Experimental setup for on resonant and light shift Rabi oscillator strength measurements

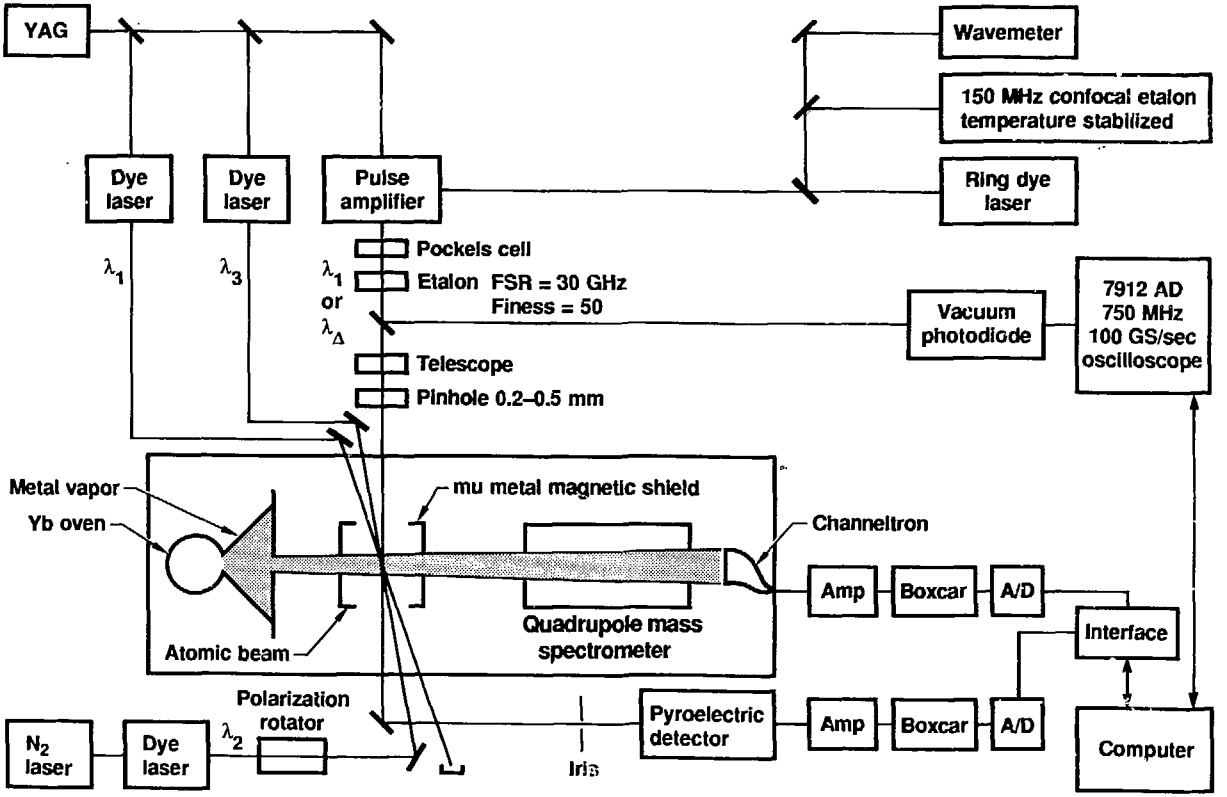

30-90-0687-6075

Fig. 2

Time dependent state populations used for on resonant Rabi oscillation experiments

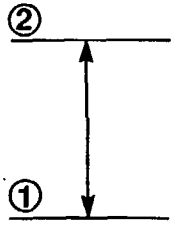

$J = 1,\ m_j = 0$

$\Omega_{12} = \frac{pE(t)}{2\hbar}$ Two level atom — on resonance

$J = 0\ \ m_j = 0$

$$\begin{pmatrix} \dot{C}_1 \\ \dot{C}_2 \end{pmatrix} = \dot{\vec{C}} = \frac{-i}{2}\begin{bmatrix} 0 & \Omega_{12} \\ \Omega_{12} & 0 \end{bmatrix}\vec{C}$$ after rotating wave approximation

let $J = \int_0^t E(t)\,dt$ and let $C_1\ (t = 0) = 1$

then: $\vec{C} = \begin{pmatrix} \cos\frac{pJ}{2\hbar} \\ -i\ \sin\frac{pJ}{2\hbar} \end{pmatrix} \Rightarrow$ population in level 2 $= \sin^2\frac{pJ}{2\hbar}$

The excited state population depends on the integral of the electric field. This can be determined from the total fluence delivered in a pulse and the temporal profile of that pulse, assuming constant phase.

30-90-0687-6076

Fig. 3

Digitized temporal profile for a single pulse obtained from a pulse amplified cw ring dye laser

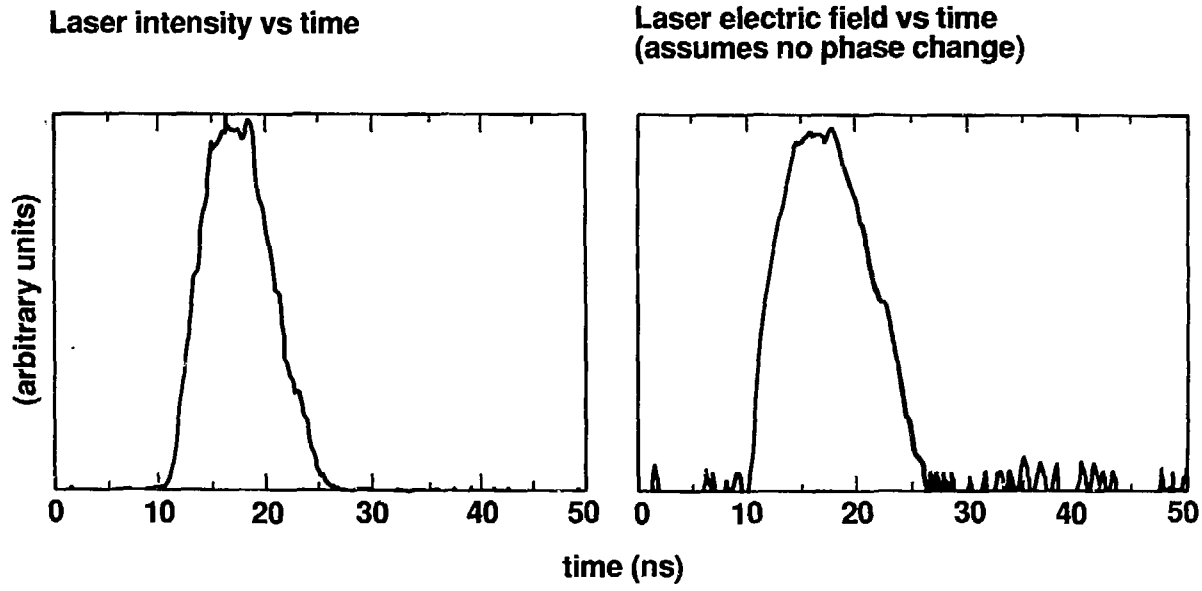

30-90-0687-6086

Fig. 4

On resonant Rabi oscillations, two level atom measurement of an oscillator strength in ^{174}Yb ($0 \Rightarrow 17992\ cm^{-1}$ $J = 0 \Rightarrow 1$, $m_j = 0 \Rightarrow 0$)

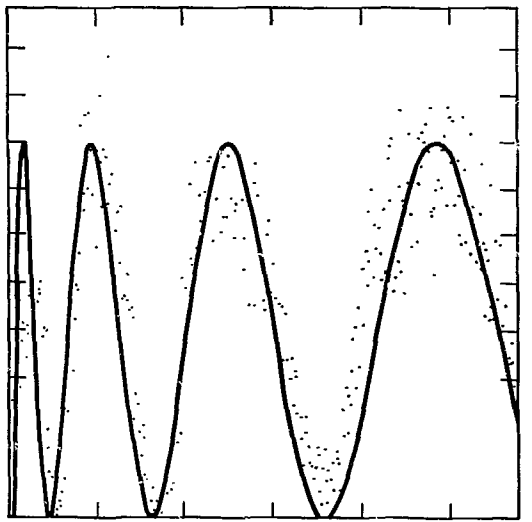

Value measured

$$f_{u\ell} = (1.82 \pm 0.36) \times 10^{-2}$$

Value derived from literature

using $\tau_{17992} = 875\ ns$[(a)]

Branching ratio = 1

$$f_{u\ell} = 1.59 \times 10^{-2}$$

[(a)]M. Gustavsson, H. Lundberg, L. Nilsson, and S. Svanberg J. Opt. Soc. Am. 69, 984 (1979).

30-90-0687-6081

Fig. 5

Photoselective ionization of Yb odd isotopes using linearly polarized light on J = 0→1→1 transition sequence

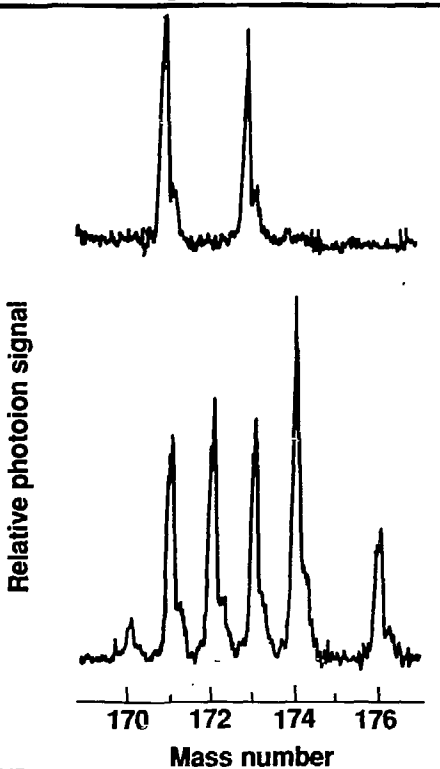

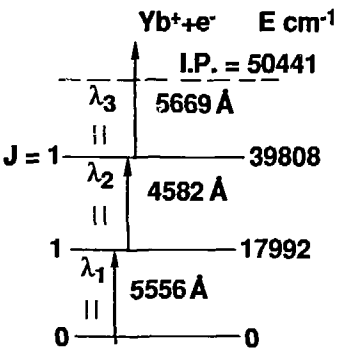

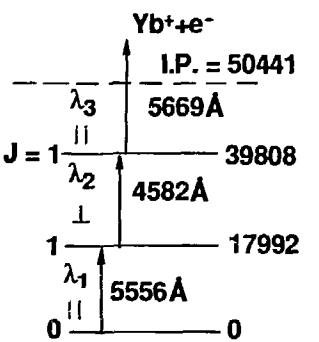

30-90-0587-1177

Fig. 6

Excitation sequence for oscillator strength measurement observing light shift Rabi oscillations

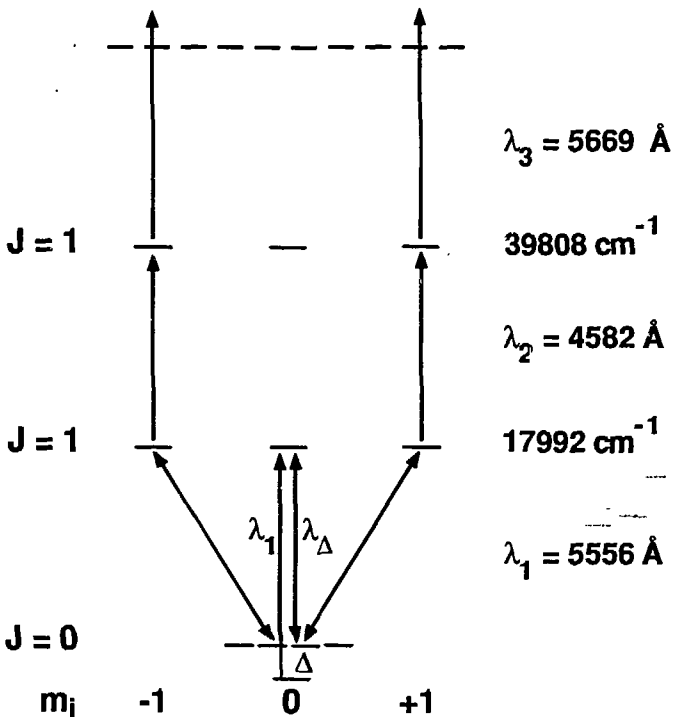

$\lambda_\Delta = \lambda_i + \Delta$

$\lambda_1, \lambda_2, \lambda_3$ linear parallel polarized

λ_1 polarization rotated 54.7° to λ_Δ

All lasers pass through vapor temporally separated

30-90-0687-6074

Fig. 7

Steps in solving for the time dependent state population oscillations caused by a light shift laser

1) Express state as originally prepared by λ_1: Quantization axis along z axis.

$$\vec{C}(t=0) = \begin{pmatrix} |-1\rangle \\ |0\rangle \\ |1\rangle \end{pmatrix} = \begin{pmatrix} 0 \\ 1 \\ 0 \end{pmatrix}$$

2) Rotate coordinate system so that quantization axis is parallel to the light shift laser's λ_Δ E-field.

$$\vec{C}'(t=0) = D^{(1)}(0, \beta, 0)\ \vec{C}(t=0)$$

$D^{(1)}(0, \beta, 0)$ = unitary representation of rotation group

3) Time evolve the amplitudes and phases of the rotated states. This is now a simple two-level atom. Use adiabatic elimination.

$$\vec{C}'(t) = \begin{pmatrix} C_{|-1'\rangle}(t=0) \\ C_{|0'\rangle}(t=0) \exp \dfrac{-i\Omega_{o',\ell}^2 t}{4\Delta} \\ C_{|+1'\rangle}(t=0) \end{pmatrix}$$

4) Rotate back into original coordinate system.

$$\vec{C}(t) = D^{(1)\dagger}(0, \beta, 0)\ \ \vec{C}'(t)$$

5) Find populations in m $= \pm 1$ levels.

$$P_{m_{-1}} = P_{m_{+1}} = C_{|+1\rangle} C^*_{|+1\rangle}$$

6-5-87 CAH-1

Fig. 8

Determine original state amplitudes in rotated coordinate system

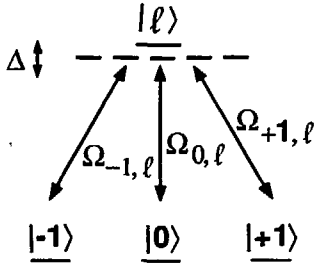

Excite λ_Δ at angle β to λ_1,

$D^{(1)}(0, \beta, 0)$

Unitary rotation matrix
z quantization → z''

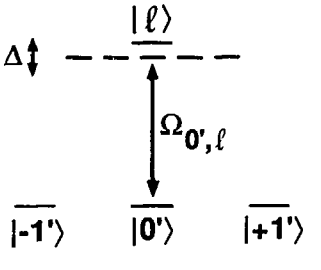

transformed states |m' >,
amplitude $\vec{C}'$

Original states |m >; amplitude $\vec{C}$
Assume all population originally resided in |0⟩
Calculate rotated amplitudes

$$\vec{C}'(t=0) = D^{(1)}(0, \beta, 0)\,\vec{C}\,(t=0) = \begin{pmatrix} \frac{1+\cos\beta}{2} & \frac{-\sin\beta}{\sqrt{2}} & \frac{1-\cos\beta}{2} \\ \frac{\sin\beta}{\sqrt{2}} & \cos\beta & \frac{-\sin\beta}{\sqrt{2}} \\ \frac{1-\cos\beta}{2} & \frac{\sin\beta}{\sqrt{2}} & \frac{1+\cos\beta}{2} \end{pmatrix} \begin{pmatrix} 0 \\ 1 \\ 0 \end{pmatrix}$$

$$\vec{C}'(t=0) = \begin{pmatrix} \frac{-\sin\beta}{\sqrt{2}} \\ \cos\beta \\ \frac{\sin\beta}{\sqrt{2}} \end{pmatrix}$$

30-90-0687-6078

Fig. 9

Time evolution of state amplitudes in rotated coordinate system after adiabatic elimination of $C_{|2'>}$

$$\dot{\vec{C}'} = \begin{pmatrix} \dot{C}_{|0'>} \\ \dot{C}_{|\ell>} \end{pmatrix} = -\frac{i}{2} \begin{bmatrix} 0 & \Omega_{0',\ell} \\ \Omega_{0',\ell} & 2\Delta \end{bmatrix} \vec{C}'$$

$C_{|\ell>}$ oscillates rapidly with respect to $C_{|0'>}$ so integrate $C_{|\ell>}$ holding $C_{|0'>}$ constant

$$\dot{C}_{|\ell>} = -\frac{i}{2}\left(C_{|0'>}\,\Omega_{0',\ell} + C_{|\ell>}\,2\Delta\right) \Rightarrow C_{|\ell>} = \frac{C_{|0'>}\,\Omega_{0',\ell}}{2\Delta}\,[\exp(-i\,\Delta\,t) - 1]$$

The exponential oscillates rapidly about zero and can be eliminated if $\Delta \gg \Omega_{0',\ell}$

$$\overline{C}_{|\ell>} = -C_{|0'>}\,\Omega_{0',\ell}/2\Delta$$

so,

$$\dot{C}_{|0'>} = -\frac{i}{2}\Omega_{0',\ell}\,C_{|\ell>} = \frac{i\,\Omega^2_{0',\ell}}{4\Delta}\,C_{|0'>}$$

$$C_{|0'>}(t) = C_{|0'>}(t=0) \quad \exp\left[\frac{-i\,\Omega^2_{0',\ell}\,t}{4\Delta}\right]$$

6-5-87 CAH-2

Fig. 10

Rotate back to original coordinates and solve for populations

$$\vec{C}(t) = D^{(1)\dagger}(0,\beta,0)\,\vec{C}'(t) = \begin{pmatrix} \frac{\sin\beta\cos\beta}{\sqrt{2}} & \left[\exp\left(\frac{-i\,\Omega^2_{0',\ell}\,t}{4\Delta}\right) - 1\right] \\ \sin^2\beta + \cos^2\beta & \exp\left(\frac{-i\,\Omega^2_{0',\ell}\,t}{4\Delta}\right) \\ \frac{\sin\beta\cos\beta}{\sqrt{2}} & \left[1 - \exp\left(\frac{-i\,\Omega^2_{0',\ell}\,t}{4\Delta}\right)\right] \end{pmatrix}$$

so, $C_{|+1>}C^*_{|+1>} = \sin^2\beta\,\cos^2\beta\left[1-\cos\frac{\Omega^2_{0',\ell}\,t}{4\Delta}\right] = P(t)$

but, $\Omega^2_{0',\ell} = \frac{1}{\pi}\left(f_{\ell u}\,\hat{I}\left[\frac{\text{photons}}{\text{cm}^2\,\text{sec}}\right]\right)$ and let $I\left[\frac{\text{photons}}{\text{cm}^2}\right] = \int_0^t \hat{I}\,dt$

Then, $P_1(I) = \sin^2\beta\,\cos^2\beta\left[1-\cos\frac{f_{\ell u}\,I}{4\pi\Delta}\right]$ $\qquad [\Delta] = \text{rad/sec}$

for $J = 1 \rightarrow J = 0$

$f_{\ell u} = \frac{1}{3}\,f_{u\ell} = \frac{8\pi^2\Delta\,n}{I}$

n = number of oscillation periods of oscillation at fluence I

6-5-87 CAH-3

Fig. 11

Time dependence of state populations as a function of laser detuning, light shift Rabi oscillations, exact solutions

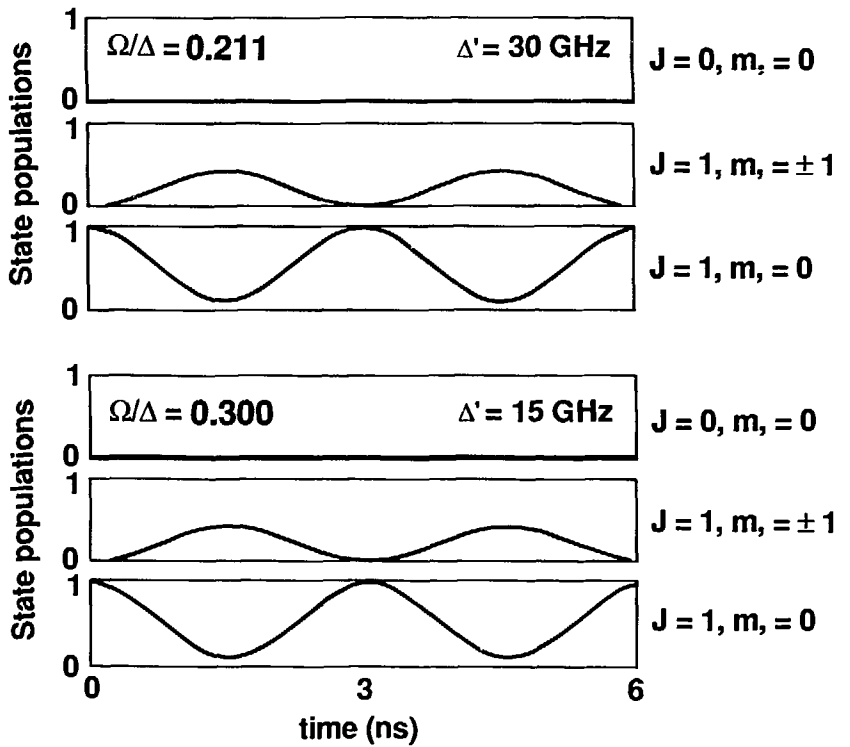

Laser intensity constant throughout pulse and adjusted to give two cycles in adiabatic approximation

$\Delta = 2\pi\,\Delta'$

$\beta = 54.7^{c}$

30-90-0687-6084

Fig. 12

Time dependence of state populations as a function of laser detuning, light shift Rabi oscillations, exact solution

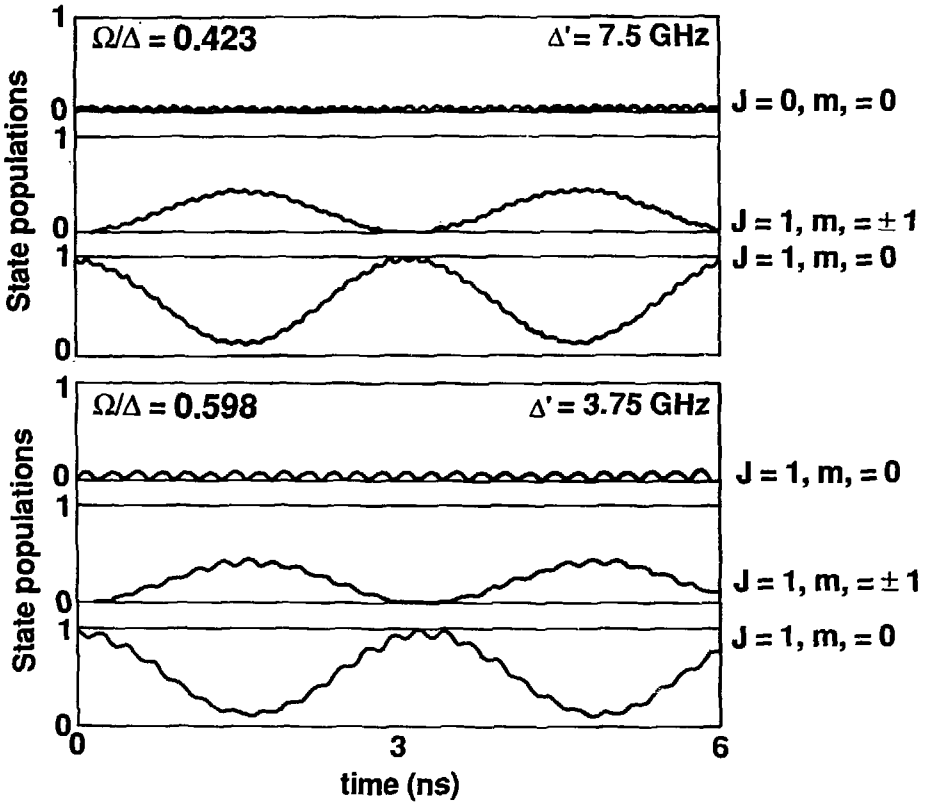

Laser intensity constant throughout pulse and adjusted to give two cycles in adiabatic approximation

$\Delta = 2\pi\,\Delta'$

$\beta = 54.7^{\circ}$

Fig. 13

Time dependence of state populations as a function of laser detuning, light shift Rabi oscillations, exact solutions

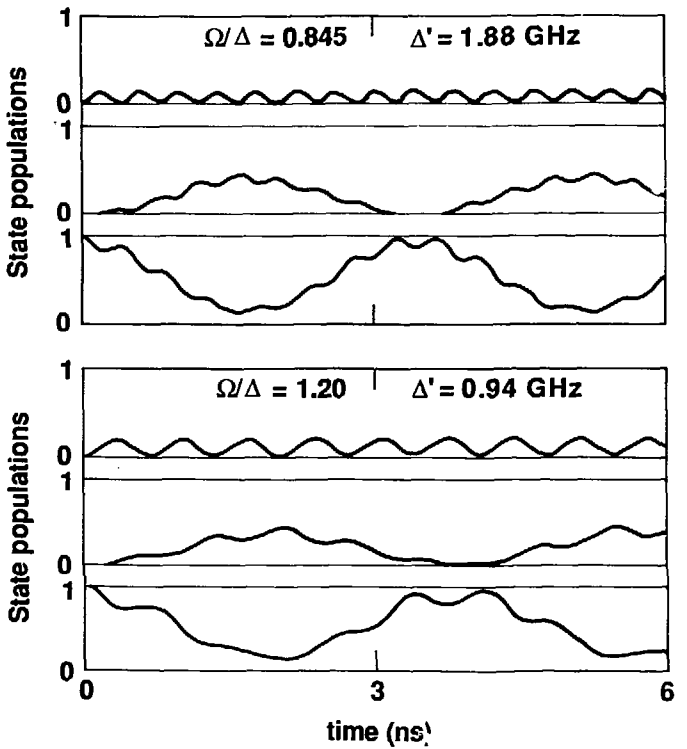

Laser intensity constant throughout pulse and adjusted to give two cycles in adiabatic approximation

$\Delta = 2\pi\,\Delta'$

$\beta = 54.7°$

30-90-0687-6082

Fig. 14

Light shift Rabi oscillations (inverse hook method) vs detuning measurement of an oscillator strength in ^{174}Yb 17992 $\Rightarrow$ 0 cm^{-1}, J = 1 $\Rightarrow$ 0

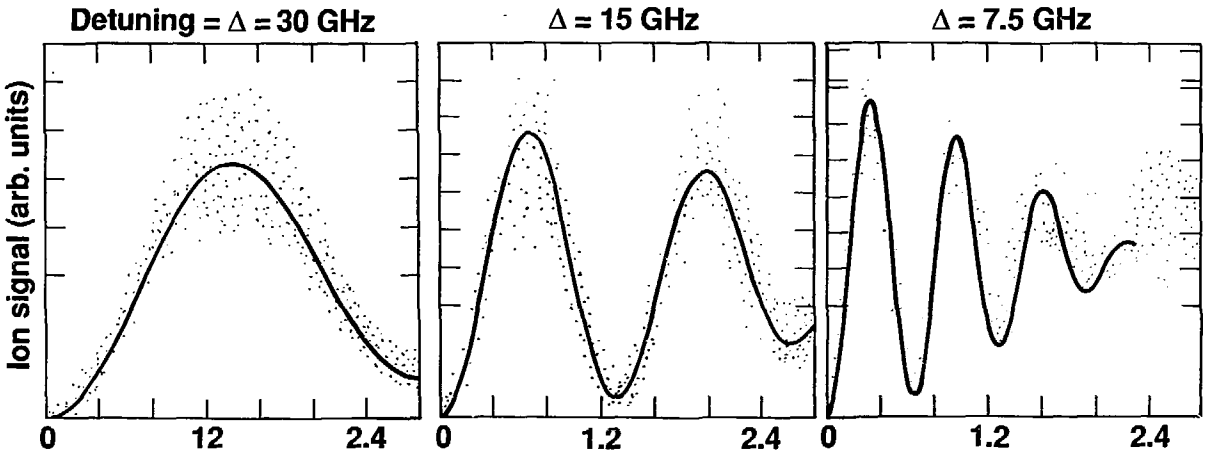

Fits to data (solid line) give $f_{\ell u} = (0.52 \pm 0.1) \times 10^{-2} \Rightarrow f_{u\ell} = (1.57 \pm 0.31) \times 10^{-2}$

Fig. 15